A Stochastic, Local Mode Treatment of High-Energy Gas−Liquid Collisions†

Daniel M. Packwood and Leon F. Phillips*

Chemistry Department, University of Canterbury, Christchurch, New Zealand

Received: December 17, 2008; Revised Manuscript Received: April 6, 2009

The scattering angle distributions of high-energy molecular beams at the surfaces of three different liquids are treated in terms local mode theory. This is achieved by setting up a stochastic process modeling the effect of a superposition of local mode surface displacements on the incoming particle's trajectory. The results are found to be in good qualitative agreement with experiment, and directions for further work are indicated.

1. Introduction

It is often fruitful to consider the gas−liquid interface within the continuum regime, even when events on the scale of individual molecules are of interest. The usual approach is through capillary wave theory, which was introduced by Buff, Lovett, and Stillinger in 1965.[1] The interface is regarded as a dividing surface, at which the bulk liquid-phase density undergoes a sharp transition to gas-phase values and whose location has a normal distribution around 0 displacement. The theory assumes that displacements of this surface from its average position are restored by the liquid's surface tension and that their variation with distance along the surface can be represented by a Fourier series of sine or cosine functions, which constitute the "capillary waves" of the theory. This form of capillary wave theory is conceptually satisfying and has had modest success in modeling reflectivity data,[2] but it falls short of explaining some important interfacial phenomena such as surface roughness[3−5] and interfacial width.[6]

At very short wavelengths, the sine or cosine functions lose their physical significance because the component waves are damped by viscosity at a distance much shorter than one wavelength; therefore, the component waves are merely one of many mathematical basis sets that could be used to describe the shape of the surface displacement as a function of distance along some arbitrary axis.[7] Solutions of the Navier−Stokes equation in this "local mode" regime can be obtained in the form of Bessel functions, with arbitrary displacements of the dividing surface being expressed as a Fourier−Bessel series.[2,8−10] Thus, the local mode theory describes small-scale displacements of the surface as a superposition of Bessel functions. The basic idea is that small-scale surface disturbances occur when the thermal motion of molecules or small groups of molecules at and below the surface produce a sudden, localized, positive or negative displacement of the surface. When the wave equation is set up in this framework, Bessel functions are obtained as the radial solution for the surface displacement,[2] and it can be shown[9] that a single local mode displaces the dividing surface by a distance

$$\varepsilon(r) = \text{constant} \times c(t) J_0(kr) \qquad (1)$$

after time t from the initial impact, where $J_0(kr)$ is the Bessel function, r is the radial distance from the center of the displacement, and

$$c(t) = \exp\left(-\frac{2k^2\eta}{\rho}t\right) - \exp\left(-\frac{k\gamma}{2\eta}t\right) \qquad (2)$$

Here, η, ρ, and γ are the viscosity, density, and surface tension, respectively, of the liquid. The quantity k, which corresponds to the wave vector of capillary wave theory, is inversely proportional to the width of the displacement and controls the rate of rise and decay of the local mode; the most rapid displacements are also the most narrow. At the large values of k that are relevant to this study, $2k^2\eta/\rho \gg k\gamma/2\eta$, so that a local mode displacement is characterized by a rapid rise, followed by a much slower fall. The root-mean-square (rms) displacement of a point on the dividing surface, with k averaged over all values between the transition to local modes and the upper limit set by the molecular diameter, is estimated to be 2−3 Å for typical liquids,[2] which sets 12−18 Å as approximate bounds (3 rms displacements or 99% confidence limits for locating the dividing surface) on the interfacial width. If we confine our attention to the largest values of k, these ranges are correspondingly smaller. In practice, we shall use interfacial widths provided by molecular dynamics simulations (see Table 1), which, at present, are limited to short time scales and high k values.

Local mode theory has been successful in accounting for small-scale surface roughness measurements[10] but still requires testing against other experimental data. Here, we show that local mode theory predicts scattering angle distributions of atoms from liquid surfaces that are in reasonable agreement with high-energy molecular beam data obtained below the specular angle when the Bessel function bases are explicitly considered as the scatterers. To achieve this, we employ a simplified model which assumes that the incoming particles are of sufficiently high

TABLE 1: Parameters Used in the Scattering Angle Calculations

	glycerol (298 K)	squalane (290 K)	PFPE (290 K)
θ_i (degrees)	50[18]	65[12]	65[12]
w (Å)	4.0[21]	6.0[22a]	5.0[d]
ρ (g cm^{-3})	1.26[11]	0.81[11]	1.90[25c]
η (mPa s)	1400[11]	34[23b]	490[25c]
γ (mN m^{-1})	63[11]	26[24]	19[e,c]

[a] Estimate at 298 K (Kohler et al.[22]). [b] Estimated at 0 external pressure from three measurements at different external pressures (Table 4, listing $x = 0$, in Tomida et al.[23]). [c] Value at 293 K. [d] Average of glycerol and squalane values. [e] Value for DuPont Krytox 1525, which has a similar density and viscosity as Krytox 1625 PFPE.[26]

† Part of the "Robert Benny Gerber Festschrift".

* To whom correspondence should be addressed.

10.1021/jp811164u CCC: $40.75
Published on Web 04/22/2009

energy that the effect of the gas−liquid interaction potential on the beam's trajectory can be ignored and that the particles scatter elastically from the surface. The latter assumption will appear severe to anyone familiar with the field because it is well-known that even high-energy particles undergo extensive energy transfer upon colliding with a liquid surface.[11] However, it is also known from experimental[12] and simulation studies[13] that the shapes of scattering angle distributions of high-energy beams essentially derive from the geometry of the surface itself. Our model involves formulation of a stochastic process describing which local mode on the surface intersects the molecular beam at time t and obtains the most probable angle of deflection of the beam from the slope of the local mode at the intersection. Since the underlying model is simplified to the extent that it does not account for inelastic or low-energy scattering, this work is possibly best regarded as a test of local mode theory.

2. Methods Section

2.1. Basic Equations. In its original form, local mode theory presents some mathematical complications which require approximation. We restrict the analysis to two dimensions (horizontal along the surface and vertical across the density profile), which is adequate for modeling experimental in-plane scattering distributions. This is possible because the local modes responsible for the scattering must be centered on the plane containing the beam, the point of impact on the surface, and the detector. If a local mode were centered slightly out of this plane, scattering would occur on either side of the plane and would not be seen by the detector. Since the shape of the displacements in eq 1 will be difficult to handle when developing a simple probability law for the stochastic process (see section 2.2) and the fact that eq 1 will need to be solved for the argument kr, we use Newman's parabolic approximation for the Bessel function[14]

$$J_0(kr) = 1 - \frac{1}{4}k^2r^2 \tag{3}$$

This approximation holds for $-2.405 \leq kr \leq 2.405$, which implies that all scattering occurs within the first zero of the Bessel function. We set $k = 10^9$ m^{-1}, which is of the same order of magnitude as the upper limit of the k spectrum.[9] This supposes that the only significant gas−surface interactions occur with local modes of the same order of size as the incoming molecule. This assumption is rather drastic with a continuum model but is mitigated by the experimental observation that the liquid surface becomes markedly less rough near the upper limit of k.[5] Also, although there would be a bumpy atomic topology along the local mode surface at high k, these bumps would be a relatively unimportant feature of the overall local mode geometry. The essential difference between molecular beam scattering from a gas and that from a liquid is that scattering from a liquid involves the interaction of the beam particle with a number of surface and even subsurface molecules almost simultaneously, so that much of the bumpiness of the surface is averaged out. We return to this point in section 2.3. Negative-going local mode displacements are also neglected, which simplifies formulation of the stochastic process in section 2.2, at the price of eliminating a major source of multiple collisions with the surface.

With these approximations, the constant in eq 1 may be estimated. Let w be the width of the interfacial region (resulting from local modes with $k \sim 10^9$ m^{-1}) and let c_{max} be the value of $c(t)$ at the turning point of the mode. Then, as $r \rightarrow 0$ and $c(t) \rightarrow c_{max}$, $\varepsilon \rightarrow w$, by assumption. By eqs 3 and 1, this limit gives

$$\text{constant} = \frac{w}{c_{max}} \tag{4}$$

As noted above, w is to be estimated from the widths of interfacial density profiles reported in the molecular dynamics simulation literature. Since the short simulation times prevent local modes with small k from occurring, the density profile is necessarily averaged over motions corresponding to large k values. The width of such a profile should therefore correspond fairly closely to the maximum amplitude of a local mode at the upper end of the k spectrum. In addition, it seems unlikely that the short simulation times could generate a velocity potential for a substantial, negative-going displacement at the surface.

Note that, within the superposition picture, the "time" argument in $c(t)$ is not the same time that is recorded in the laboratory. Rather, it is the time since the start of the local mode's displacement from 0. Since each local mode in the superposition rises and falls independently of the others, this parameter will have a different zero for each local mode. To make the distinction clear, the argument t is replaced by s. In addition, the location a of the local mode's center relative to an arbitrary origin on the surface will be important; therefore, we need to replace r with $r - a$ in eq 3. Hence, from eqs 3, 4, and 1, the displacement of the surface by local mode a at time s into its lifetime is

$$\varepsilon_a(r, s) = w\frac{c(s)}{c_{max}}\left(1 - \frac{1}{4}k^2(r - a)^2\right) \tag{5}$$

2.2. Formulation of the Stochastic Processes. To model the effect of a superposition of local modes, each evolving according to eq 5 with distinct a and various s, on the incoming particle's trajectory, we formulate the stochastic process (A_t,C_t), $t \in T$, which gives the local mode origin a and function $c(s)$ encountered by the incoming molecule at time t as the respective components. The stochastic processes will be distinguished from their counterparts in the preceding equations by writing them with capital Roman letters. As will be shown, specification of the probability law on (A_t,C_t) will lead to a stochastic process modeling the local mode slope encountered by the incoming particle's trajectory, which in turn is used to calculate the scattering angle at time t.

We proceed to put a realistic probability law on (A_t,C_t). Rigorously, the parameter space T should be taken as the half-line $[0, \infty)$, but for simplicity, we use the set of discrete indices $\{0, 1, 2,...\}$ and assume the time step to be vanishingly small. Consider a single projectile traveling toward the liquid surface on a fixed, straight-line trajectory, which makes an angle θ_i to the surface normal and terminates at the origin on the surface. It is assumed that once within a distance w of the surface, the trajectory is intersected by a local mode at some point into its oscillation. Let (A_0,C_0) be given as an initial condition. Then, at time $t = 1$, the trajectory will either be intersected by a new local mode with probability p or will intersect the next segment of the current local mode's oscillation, with probability $q = 1 - p$. If the former event occurs, it is required that $A_1 > A_0$ since the local mode at A_0 blocks access to modes lying behind it. It is also required that C_1 is such that the top of the local mode at A_1 has just intersected the trajectory. The probability law then continues in this fashion for $t = 2$ onward. A boundary condition is also required, for if the trajectory continues to intersect a single local mode, there will come a point where that local mode slips below the particle's trajectory. At this point, the trajectory is allowed to proceed behind that local mode, where it is intersected by a local mode with $A_k < A_{k-1}$ at a random point into its oscillation (i.e., C_k is a uniform random variable). In all

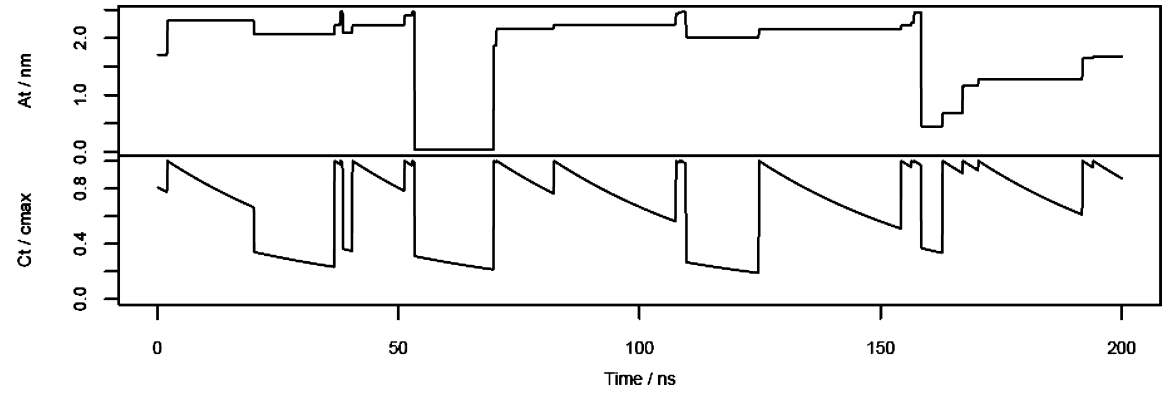

Figure 1. A representative segment of a sample path of (A_t,C_t), simulated with parameters for glycerol at 298 K (see Table 1) and $p = 0.01$. The C_t component is plotted as C_t/c_{max} to ease interpretation.

cases the domain on C_k is restricted to the segment of the oscillation for which the local mode A_k intersects the trajectory. The simplicity of this probability law results from the approximation of the Bessel function by a parabola in eq 5; the use of a convex function with compact support eliminates the need to account for the intersection of the beam by maxima beyond the center of the displacement. The parameter p essentially relates to the frequency at which new local modes intersect the beam trajectory and can be estimated by a statistical mechanical treatment of thermal fluctuations in the bulk liquid.[15] To avoid introducing more assumptions, we leave p as an adjustable parameter. The nature of the sensitivity of the calculated results to p does not suggest that this results in any serious ill-definition of the model (see section 3).

A representative segment of a sample path of (A_t,C_t) is shown in Figure 1, using parameters for glycerol at 298 K (see Table 1), $p = 0.01$, and the simulation conditions described at the end of this section. The A_t component, which identifies the local mode intersecting the trajectory at time t, is seen to undergo step-like fluctuations. When the trajectory is intersected by a new local mode in the superposition, A_t undergoes a step increase to a local mode lying in front of the previous one, and when the current local mode slips below the trajectory, A_t makes a step decrease to a local mode lying behind the previous one. The time evolution of the intersecting local mode is described by the C_t component, which also undergoes step-like fluctuations, although during each step, it follows the course of the deterministic function $c(s)$. Accordingly, when A_t undergoes a step increase, C_t takes on the first value of $c(s)$, which permits that local mode to intersect the trajectory. In this case, this value is always $\sim c_{max}$ as the rising phase of $c(s)$ is faster than the time step used in these calculations. Similarly, when A_t undergoes a step decrease, the next value taken on by C_t is a random value of $c(s)$, subject to the condition that the local mode at A_t still intersects the trajectory. Since the sample paths of the C_t component spend considerable time behaving as the classical function $c(s)$, the term "stochastic process" is being used rather loosely in this work. Note that the (A_t,C_t) depend only on the state of the current local mode intersecting the trajectory and are otherwise independent of the history of the system. This is an approximation because the long fall time of each local mode should have a prolonged influence on the trajectory. In a crude sense, the Markov assumption is being employed.

From (A_t,C_t), two more-useful stochastic processes may be specified, namely, the local mode displacement encountered at time t, defined by

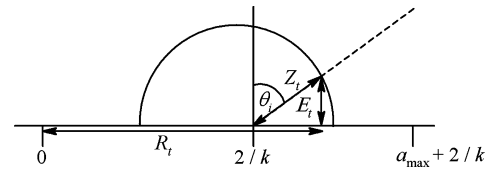

Figure 2. Calculation of E_t and R_t following the shift of the origin by $2/k$. The incoming particle's trajectory is represented by a dotted line and makes an angle θ_i to the surface normal.

$$E_t = w\frac{C_t}{c_{max}}\left(1 - \frac{1}{4}k^2(R_t - A_t)^2\right) \tag{6}$$

and the local mode slope encountered at time t, given by

$$G_t = \frac{-wk^2C_t}{2c_{max}}(R_t - A_t) \tag{7}$$

(i.e., the partial derivative of eq 5 with respect to r, as a stochastic process), where R_t is the distance along the horizontal axis from origin to the point on the local mode encountered at time t. In order to achieve this, we show that R_t is a well-defined function of (A_t,C_t). First, observe that all local modes from $-2/k$ from the origin to some distance a_{max} may intersect the trajectory. This follows since, under Newman's approximation, $kr = -2$ at the intersection of the horizontal axis for all $c(s)$. Now, assume that the local mode at a_{max} can only intersect the trajectory at $r - a = 0$ and $c(t) = c_{max}$ (i.e., at full displacement). Let y be the distance from the origin to the top of this local mode when it is fully displaced. Then, by these arguments and eq 5, $w = y\sin(\pi/2 - \theta_i) = y\cos\theta_i$ and $a_{max} = y\cos(\pi/2 - \theta_i) = y\sin\theta_i$, which gives $a_{max} = w\tan\theta_i$. Next, it will prove fruitful to shift the origin by $2/k$ units, such that the trajectory now terminates at point $2/k$ on the surface and that all local modes between $a_{max} + 2/k$ and 0 may intersect the trajectory. From Figure 2, it is evident that E_t and R_t are

$$E_t = Z_t\sin(\pi/2 - \theta_i) = Z_t\cos\theta_i \tag{8}$$

and

$$R_t = Z_t\cos(\pi/2 - \theta_i) + 2/k = Z_t\sin\theta_i + 2/k \tag{9}$$

respectively, where Z_t is the distance from point $2/k$ on the surface (the old origin) to the part of the trajectory struck by the local mode at time t. Substituting eqs 8 and 9 into eq 6 gives

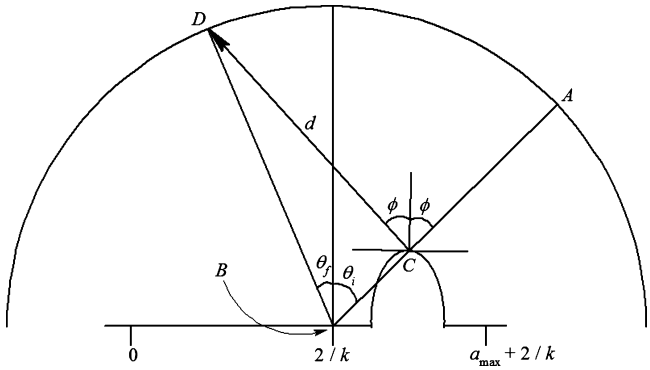

Figure 3. Calculation of the final scattering angle θ_f. The particle's trajectory, *AB*, is intersected by a rising local mode at point *C*. The trajectory is reflected along a tangent to the point encountered on the local mode (given by G_t), producing the reflected trajectory *CD*. The detector moves along the outer semicircle and is assumed to be such a great distance from the surface that *d*, the length of *CD*, is essentially the radius of the semicircle. θ_f is then calculated from elementary trigonometric considerations. The local mode is not drawn to scale for clarity.

$$0 = Z_t^2 \sin^2\theta_i + Z_t\left\{2\left(\frac{2}{k} - A_t\right)\sin\theta_i + \frac{4c_{max}\cos\theta_i}{wk^2C_t}\right\} - \frac{4A_t}{k} \quad (10)$$

When $A_t = 2/k$, the acceptable solution must go to 0 as $C_t \rightarrow 0$, which is satisfied by the positive solution of eq 10. Because of its length, this solution will not be quoted here. With this expression for Z_t in terms of A_t and C_t, eqs 9, 6, and 7, E_t and G_t are fully specified.

All of the calculations reported here simulate (A_t,C_t) for 10^6 time steps of 0.1 ns length, with each local mode separated by a distance $a_{max}/500$, and initial conditions $A_0 = -2/k$ and $C_0 = c_{max}$. In every case, output from the first 100 time steps has been removed to avoid possible spurious behavior during the early stages of the simulation. All calculations were performed with R 2.4.1,[16] and all codes are available upon request.

2.3. Calculating the Scattering Angle Distribution. The encountered slope G_t is used to calculate an elastic scattering angle distribution by reflecting a unit vector coincident to the molecular beam across a tangent to the surface, assuming a structureless, spherical projectile. Our approach is shown diagrammatically in Figure 3. The distribution is constructed as a histogram of the scattering angles θ_f produced by the sample path of G_t. Since discussion of the following results does not require the cumbersome equations produced by this method, their derivations are left to the Supporting Information. The large number of time steps (10^6) used in simulating (A_t,C_t) ensures that the predicted scattering angle distributions are not affected by the variance of the (A_t,C_t) sample paths, which was found to have a noticeable effect for simulations using fewer than $\sim 10^3$ time steps.

In this treatment, θ_f will never exceed the specular angle (where $\theta_f = \theta_i$). This occurs because, in putting a probability law on (A_t,C_t), it was assumed that the very top of a rising local mode is the first segment to intersect the projectile's trajectory when the trajectory changes to a new mode, and an incoming particle can only ever collide with the very top of the local mode or the side closer to the incoming molecule. This restricts G_t to 0 or negative values (i.e., in eq 7, $R_t - A_t \geq 0$ for all t), which in turn only allows reflection at or below the specular angle. This is an approximation because, for all $a \geq 2/k$, the first part of the rising local mode to intersect the trajectory will be a small segment on the side further from the incoming molecule, even in the absence of an attractive potential. For a beam striking a glycerol surface, the most negative slope that could be encountered would occur on a fully displaced local mode centered at 0, which gives a lower-bound slope and scattering angle of −0.4 and 6.4° for all incident angles. This lower-bound to the scattering angle is representative of all systems studied here. In addition, our neglect of a gas−liquid potential interaction prevents the beam from diverting into the back side of the local mode at close range, as is the normal occurrence with scattering from the point source of an interaction potential, which would produce more scattering beyond the specular angle. As mentioned in section 2.1, molecular-scale local modes would have a bumpy atomic topology along the curve in eq 5. The local

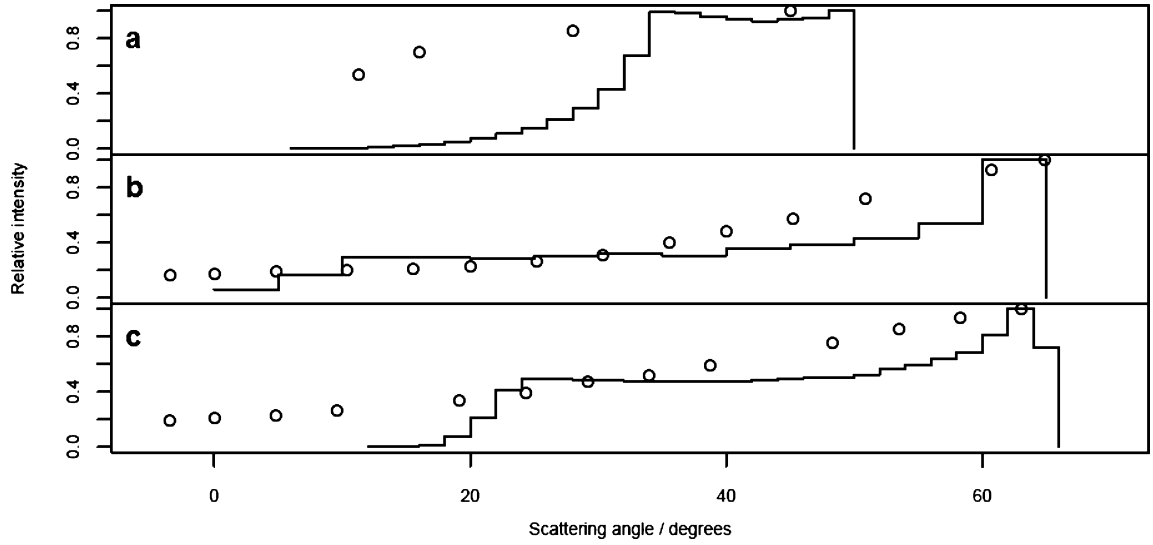

Figure 4. Scattering angle distributions predicted by the stochastic processes (steps) with experimental measurements from high-energy beams overlaid as points for (a) a glycerol surface at 298 K with $p = 0.0038$ (measurements by Sinha and Fenn with a 43 kJ mol^{-1} Ar beam[18]), (b) a squalane surface at 290 K with $p = 0.04$ (measurements by King et al. with a 185 kJ mol^{-1} Xe beam[12]), and (c) a PFPE surface at 290 K (measurements by King et al. with a 185 kJ mol^{-1} Xe beam[12]) with $p = 0.0026$. Although not shown, experimental measurements have been reported beyond the specular angle in each case; see section 2.3.

modes considered here have widths of 4 nm and full heights between 4 and 6 Å, whereas for, say, a hydrocarbon liquid, the atomic bumps would extend above the local mode curve by the radius of a carbon atom (~0.77 Å) at most. Furthermore, the fluid molecules considered in this study are very large on the scale of the incoming particle and will tend to be aligned with the surface during the collision event. Hence, the bumps can be regarded as a small perturbation on the overall local mode geometry, and their effect would largely be averaged out as a result of the impact of a collision being spread over a significant area of the surface. Nevertheless an incoming particle would be exposed to a range of slopes, which would broaden the scattering distribution about the specular angle to some extent. We also neglect the possibility of a particle undergoing multiple reflections in the well between two modes, which might result in the particle appearing to skid along the surface.[17] Experimental scattering distributions of high-energy beams do rapidly decrease beyond the specular angle;[12,18,19] therefore, by examining the consistency between experimental and predicted scattering distributions below the specular angle, we can assess the quality of the local mode picture of the liquid surface.

3. Results and Discussion

Figure 4 shows scattering angle distributions predicted by the encountered slope G_t for a glycerol surface at 298 K, a squalane surface at 290 K, and a PFPE (DuPont Krytox 1625 perfluorinated polyether) surface at 290 K, with experimental points corresponding to measurements by Sinha and Fenn[18] and King et al.[12] Table 1 lists the parameter values used in each calculation. Sinha and Fenn and King et al. used noble gas beams, which are appropriate for comparison with the present theory. Furthermore, the plotted results were those obtained with the most energetic beams by these researchers (a 43 kJ mol^{-1} Ar beam for Sinha and Fenn and a 185 kJ mol^{-1} Xe beam for King et al.). The measurements by Sinha and Fenn and King et al. used incident angles of 50 and 65°, respectively, relative to the surface normal. The optimal values of p were chosen by manual adjustment until the predicted distribution most closely matched the experimental distribution. Note that the interfacial widths in Table 1 are consistent with the widths anticipated from the root-mean-square displacement arguments in the Introduction. Quite a lot of data from molten metal surfaces is available,[19,20] but they have not been considered in this study because eq 1 applies only when $k \gg \rho\gamma/\eta^2$, which is larger than 10^9 m^{-1} for these liquids.[9]

In each case, the stochastic processes (and hence local mode theory) do a reasonable job of tracking the data with an optimal value of p. Discrepancies occur when trying to estimate the broadness of the distributions, although this does not necessarily imply serious inaccuracies in assuming the presence of local modes at the surface. For example, all three calculations predict very little density at scattering angles less than 20°, with the largest underestimation in the glycerol case. However, the beam used by Sinha and Fenn was relatively slow, which is expected to introduce a larger inelastic component into the distribution than in the case of the results of King et al. due to the greater influence of the potential on the trajectory and the more likely occurrence of multiple collisions and trapping desorption of the incoming particles at the surface. This suggests that in the general case, scattering density below ~20° represent trajectories which are strongly affected by the potential and energy exchange at the surface and which are not properly accounted for by the stochastic processes. Similarly, the predicted distributions for squalane and PFPE peak sharply at the specular angle, underestimating density between 40 and 60°. These discrepancies are to be expected on the basis of the reasoning presented at the end of section 2.3. Indeed, Muis and Manson,[27] who successfully modeled rare gas scattering from molten metal surfaces with a gas−solid surface scattering model, required account of the gas−surface potential to broaden their predicted distributions and match experimental data; therefore, one might anticipate such discrepancies to be apparent with the assumptions made here. Nevertheless, the essential features of high-energy gas−liquid scattering distributions, namely, a long tail leading to a peak at the specular angle, are reproduced reasonably well by the simplified model, suggesting that the local mode picture of the liquid surface holds on the scale of a gas−liquid collision event. In molecular terms, this pictures the topology of a liquid surface as an irregular, rolling landscape of molecules piled above the bulk fluid phase in parabolic-shaped clusters, owing to their correlated motions. This picture supplements the commonly used concept of a "corrugated" liquid surface,[12] a notion which, on its own, is more natural in the context of a bumpy, ordered solid surface rather than an irregular and dynamic liquid surface.

The glycerol, squalane, and PFPE data were fitted with p values of 0.0038, 0.04, and 0.0026, respectively, which is straightforward to justify because p essentially measures the frequency at which new local modes intersect the trajectory. Glycerol and PFPE are highly viscous fluids (viscosities of 1400 and 490 mPa s); therefore, we would expect most thermal motions from the bulk to be damped well before reaching the interface, which would reduce the frequency of new local modes and hence give a very small p. With a viscosity of 34 mPa s, squalane is considerably less viscous than the above fluids, permitting more thermal motions to reach the interface and hence increasing the value of p. Since the correlation between p and viscosity is not perfect, it is likely that p is also a function of other fluid parameters. Figure 5 shows representative sample paths of E_t, the surface displacement experienced by the incoming particle's trajectory at time t, for glycerol, squalane, and PFPE, as computed with these values of p. For glycerol and PFPE, the beam spends considerable time scanning the falling phases of the local modes. However, for the squalane case, the beam is frequently intersected by new local modes. This shows that the high-energy scattering distributions from glycerol and PFPE are largely the result of the intersection of a single local mode with each incoming particle's trajectory, whereas for squalane, the distributions result from a succession of many local modes on the same trajectory. In terms of the motions of the interfacial molecules, this result can be interpreted to mean that the frequency of new molecules arriving at a unit area of a squalane surface is considerably larger than that at a unit area of a glycerol or PFPE surface. Consequently, the high-energy scattering angle distributions of PFPE or glycerol would be attributed to more so by the intersection of the trajectory by a single group of molecules rather than a rapid succession of different, independent groups of molecules. In this sense, the origins of the experimental scattering angle distributions could be partly attributed to the dynamics of bulk surface energy exchange for the liquid under consideration.

A possible criticism of this work is that leaving p as an adjustable parameter permits too much leeway in producing a scattering angle distribution. The nature of the sensitivity of the distributions to p does not suggest that this is an issue. As p tends toward unity, the beam is rapidly intersected by new local modes with successively larger displacements and spends almost all of its time reflecting from the flat, top parts of the local mode. This causes the scattering angle distributions to cluster very tightly about the specular angle at large p. As p decreases from unity, the amount of specular reflection de-

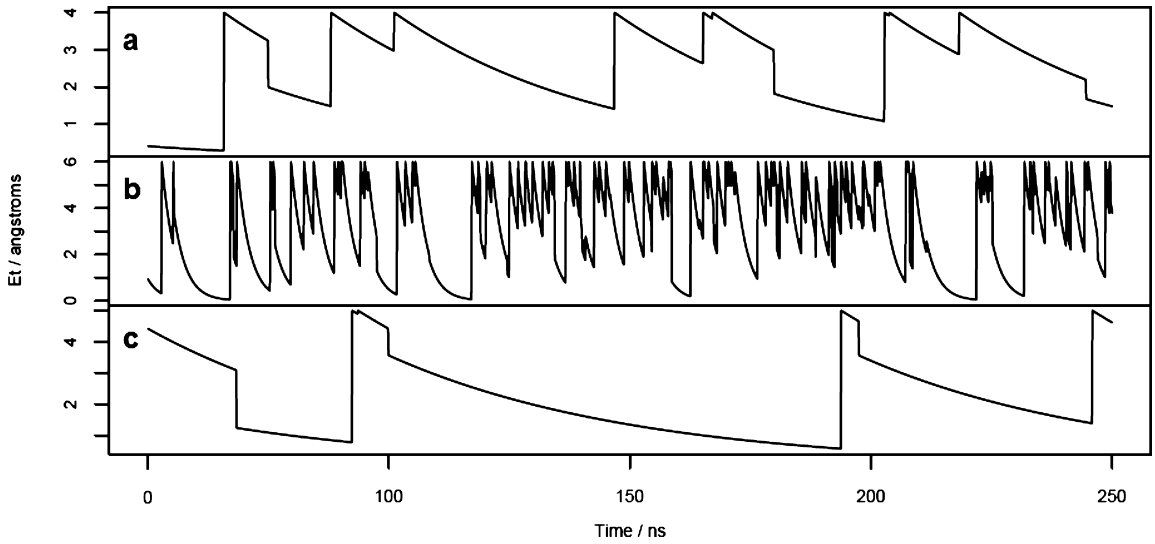

Figure 5. Representative sample paths for E_t for (a) glycerol at $p = 0.0038$, (b) squalane at $p = 0.04$, and (c) PFPE at $p = 0.0026$. E_t should be interpreted as the surface displacement experienced by the incoming particle's trajectory at time t.

creases, and the distributions adopt a wide, bell shape centered at approximately 20° below the specular angle. As p is decreased further to a critical value, the distributions rapidly take on the distinct left-skewed shape of an experimental distribution. As p approaches 0, the beam spends considerable time scanning the top of a flat, decaying local mode ($C_t \sim 0$), and the distributions narrow tightly about the specular angle once again. The observation that p induces only two distinct scattering regimes which converge to the same result suggests that the surface tension, density and viscosity carry the essential information of the model, and that by leaving p as an adjustable parameter, the model does not become ill-defined and overly dependent on p. This result is not unexpected because these three parameters implicitly account for the temperature of the fluid and the mass of the surface molecules, two features which are not explicitly accounted for in the above formulation but are known to affect experimental scattering angle distributions.[11,12] The correspondence found between the measured scattering distributions and those predicted by the stochastic processes gives some experimental support to the picture of the gas−liquid interface provided by local mode theory.

4. Conclusions

It has been shown that local mode theory can provide reasonable predictions of the scattering distributions of high-energy beams of atoms incident upon liquid surfaces. In doing so, the Bessel function bases were explicitly treated as the scatters. This permitted a probabilistic framework to be used, without significant loss of rigor, in place of the intractable deterministic framework which would be required if the dynamics of the Bessel function superposition were considered as a whole. The results in Figure 4 are qualitatively correct in that they show a steady increase in intensity up to the angle corresponding to specular reflection. The disagreement at small scattering angles is explicable in terms of a contribution from inelastic events and low-energy exit trajectories, and as would be expected, the disagreement is greater for lower-energy beams. The actual shape of the plots, with a definite plateau at medium deflection angles, does not agree with experimental data. As well as the neglect of a gas−liquid potential and atomic-size "bumps" at the local mode surface, this might also be a consequence of our choice of the parabolic approximation to a Bessel function as the two-dimensional shape of a local mode. At long times, any arbitrary displacement of the surface eventually comes to resemble a Gaussian dome,[9] whose slope decreases with increasing distance from the center of the disturbance. Such a decrease could well be expected to affect the shape of the scattering curves by reducing the intensity at medium-to-large scattering angles, but the final outcome is difficult to predict, and we are still working on the problem of incorporating a Gaussian mode into these calculations.

In the present paper, the experimental high-energy scattering distributions obtained from glycerol, squalane, and PFPE surfaces have been modeled. To our knowledge, this is the first time that this has been done from first principles on the basis of a stochastic model. Scattering distributions from molten metal surfaces have previously been derived on the basis of gas−solid scattering theory,[27] which corresponds to a short beam pulse at very high impact velocity, such that surface motions of the liquid are effectively frozen, and conclusions regarding the dynamics of the gas−liquid interface cannot be drawn. In the case of glycerol and PFPE, our calculations have shown that new local modes in the superposition infrequently intersect the molecular beam trajectory, so that the angular distributions of scattered high-energy beams result mainly from the effect of single local modes on the trajectory. In contrast, new local modes frequently intersect the trajectory at a squalane surface; therefore, the angular distribution for a given trajectory results from interactions with a succession of local modes. These inferences, which are fundamentally hydrodynamic and straightforward to interpret in terms of the motions of the surface molecules, suggest the use of a more general gas−liquid scattering theory based on local mode theory. The obvious next step is to consider inelastic collisions at low energies, where the gas−surface interaction potential is important. If this is to be done on the basis of stochastic processes, the work will inevitably involve the solution of stochastic differential equations, which is the direction of our current research.

Acknowledgment. This work was supported by the Marsden Fund and by the United States National Science Foundation (EMSI Grant Number 0431512). D.M.P. is supported by a New Zealand Tertiary Education Commission Top-Achiever Doctoral Scholarship.

Supporting Information Available: Calculation of the scattering angle from the local mode's slope. This material is available free of charge via the Internet at http://pubs.acs.org.

References and Notes

(1) Buff, F. P.; Lovett, R. A.; Stillinger, F. H., Jr. *Phys. Rev. Lett.* **1965**, *15*, 621–623.
(2) Phillips, L. F. *Chem. Phys. Lett.* **2000**, *330*, 15–20.
(3) Jeng, U. S.; Esibox, L.; Crow, L.; Steyerl, A. *J. Phys.: Condens. Matter* **1998**, *10*, 4955–4962.
(4) Simpson, G. J.; Rowlen, K. L. *Chem. Phys. Lett.* **1999**, *309*, 117–122.
(5) Fradin, C.; Braslau, A.; Luzet, D.; Smilgies, D.; Alba, M.; Boudet., M.; Mecke, K.; Daillant, J. *Nature (London)* **2000**, *403*, 871–874.
(6) Tikhonov, A. M.; Mitrinovic, D. M.; Li, M.; Huang, Z.; Schlossman, M. L. *J. Phys. Chem. B* **2000**, *104*, 6336–6339.
(7) Lighthill, J. *Waves in Fluids*; Cambridge University Press: Cambridge, U.K., 1978.
(8) Phillips, L. F. *J. Phys. Chem. B.* **2001**, *105*, 1041–1046.
(9) Phillips, L. F. *J. Phys. Chem. B.* **2001**, *105*, 11283–11289.
(10) Phillips, L. F. *J. Phys. Chem. B.* **2004**, *108*, 1986–1991.
(11) Saecker, M. E.; Nathanson, G. M. *J. Chem. Phys.* **1993**, *99*, 7056–7075.
(12) King, M. E.; Nathanson, G. M.; Hanning-Lee, M. A.; Minton, T. K. *Phys. Rev. Lett.* **1993**, *70*, 1026–1029.
(13) Lipkin, N.; Gerber, R. B.; Moiseyev, N.; Nathanson, G. M. *J. Chem. Phys.* **1994**, *100*, 8408–8417.
(14) Newman, J. N. *Math. Comput.* **1984**, *168*, 551–556.
(15) There is extensive literature surrounding such treatments. See: Gardiner, C. W. *Handbook of Stochastic Methods for Physics, Chemistry and the Natural Sciences*; Springer: Berlin, Germany, 2004.
(16) R Development Core Team. *R: A Language and Environment for Statistical Computing*; R Foundation for Statistical Computing: Vienna, Austria, 2006.
(17) Nathanson, G. M. Personal communication.
(18) Sinha, M. P.; Fenn, J. B. *Proceedings of the 5th International Symposium on Molecular Beams*; Nice, France, 1975.
(19) Tribe.; Manning, M.; Morgan, J. A.; Stephens, M. D.; Ronk, W. R.; Treptow, E.; Nathanson, G. M.; Skinner, J. L. *J. Phys. Chem. B* **1998**, *102*, 206–211.
(20) Manning, M.; Morgan, J. A.; Castro, D. J.; Nathanson, G. M. *J. Chem. Phys.* **2003**, *199*, 12593–12604.
(21) Nathanson, G. M. *Annu. Rev. Phys. Chem.* **2004**, *55*, 231–255.
(22) Kohler, S. P. K.; Reed, S. K.; Westacott, R. E.; McKendrick, K. G. *J. Phys. Chem. B.* **2006**, *110*, 11717–11724.
(23) Tomida, D.; Kumagai, A.; Yokoyama, C. *Int. J. Thermophys.* **2007**, *28*, 133–145.
(24) Lafosse, M.; Dreux, M. *J. Chromatogr.* **1990**, *188*, 315–322.
(25) Bindu, V.; Smitha, K.; Predeep, T. *Mol. Phys.* **1998**, *98*, 85–84.
(26) DuPont Krytox Performance Lubricants Data Sheet. Available online at http://www2.dupont.com/Lubricants/en_US/assets/downloads/H58530_1.pdf (accessed Nov 3 2008).
(27) Muis, A.; Manson, J. R. *J. Chem. Phys.* **1999**, *111*, 730–736.

JP811164U